

1 **First insight in trace element distribution in the intestinal cytosol of two freshwater fish**
2 **species challenged with moderate environmental contamination**

3 Tatjana Mijošek^{1,*}, Vlatka Filipović Marijić¹, Zrinka Dragun¹, Nesrete Krasnići^{1,2}, Dušica Ivanković¹,
4 Zuzana Redžović^{1,3}, Marijana Erk^{1,3}

5 ¹Ruđer Bošković Institute, Division for Marine and Environmental Research, Laboratory for
6 Biological Effects of Metals, Bijenička cesta 54, 10000 Zagreb, Croatia

7 ²Present address: University of Vienna, Department of Structural and Computational Biology,
8 Campus-Vienna-Biocenter 5, 1030 Vienna, Austria

9 ³Present address: Ruđer Bošković Institute, Division of Molecular Medicine, Laboratory for
10 Bioanalytics, Bijenička cesta 54, 10000 Zagreb, Croatia

11

12 *E-mail addresses:* tmijosek@irb.hr, vfilip@irb.hr, zdragun@irb.hr, nkrasnic@irb.hr,

13 djuric@irb.hr, zredzov@irb.hr, erk@irb.hr

14

15

16

17 *Corresponding author:

18 Tatjana Mijošek, tmijosek@irb.hr

19 Laboratory for Biological Effects of Metals, Division for Marine and Environmental Research,

20 Ruđer Bošković Institute, Bijenička cesta 54, 10000 Zagreb, Croatia.

21

22 **Abstract**

23 Cytosolic distribution of six essential elements and nonessential Cd among biomolecules of
24 different molecular masses was investigated in the intestine of brown trout (*Salmo trutta*) from
25 the karst Krka River and Prussian carps (*Carassius gibelio*) from the lowland Ilova River. Fish
26 were sampled at two locations (reference and contaminated) and in two seasons (autumn and
27 spring). Analyses were conducted by size exclusion high performance liquid chromatography
28 and high resolution inductively coupled plasma mass spectrometry. Although studied salmonid
29 and cyprinid fish have different biological characteristics, obtained profiles often showed mostly
30 similar patterns in both species. Specifically, Cd and Cu were dominantly bound to
31 metallothioneins in both species, but the same association was not observed for Zn, whereas Mo
32 distribution was similar in the intestine of both fish species with two well shaped and clear peaks
33 in HMM (100-400 kDa) and VLMM (2-8 kDa) range. In brown trout, Se was mostly associated
34 with biomolecules of very low molecular masses (VLMM, <10 kDa), whereas significant
35 additional elution in HMM region (30-303 kDa) was observed only in Prussian carp. Iron
36 binding to VLMM biomolecules (1.8–14 kDa) was observed only in brown trouts, and of Zn in
37 Prussian carps. Cobalt was mostly bound to HMM biomolecules (85-235 kDa) in brown trout
38 and to VLMM biomolecules (0.7-18 kDa) in Prussian carp. Comparison of intestinal profiles
39 with previously published data on liver and gills revealed some similarities in distribution, but
40 also organ-specific differences due to the different function and composition of each organ. As
41 so far there is no published data on intestinal trace metal distribution, the obtained results
42 represent the novel findings, and the key point for the exact identification of specific metal-
43 binding biomolecules which could eventually be used as biomarkers of metal exposure or effects.

44 **Keywords:** SEC-HPLC, brown trout, Prussian carp, HR ICP-MS, metal detoxification,
45 wastewaters

46

47

48

49

50

51

52

53

54

55

56

57

58

59

60

61

62 **1. Introduction**

63 Although essential metals have a significant role in variety of physiologically important
64 processes, often as cofactors of a number of metalloproteins and enzymes (Holm et al., 1996),
65 they can also be the cause of toxic effects if present in high concentrations. Elements as Cd or
66 Pb, considered as non-essential, do not have any known biological role in organisms and can be
67 toxic even in very low concentrations. However, commonly applied procedure of measuring only
68 total concentrations of trace elements in bioindicator organisms and their tissues does not
69 provide complete and reliable information on bioavailability, biological effects and toxicity of
70 metals in aquatic environments as their real impact is mostly connected with binding to essential
71 molecules such as enzymes or transporter proteins and their possible inactivation in the cytosol
72 (Mason and Jenkins, 1995). Cytosolic metal fraction, soluble and metabolically available,
73 consists of heat denaturable proteins (HDP, such as enzymes) and microsomes (biologically
74 available and partially toxic metal fraction), and heat-stable proteins (HSP, such as
75 metallothioneins) (detoxified metal fraction) (Wallace et al., 2003). In cytosol, metal toxic
76 effects include blocking of functional groups of biomolecules, substitution of essential elements,
77 and formation of reactive oxygen species (ROS) which have an important role in oxidative stress
78 However, they can also be detoxified either through sequestration in forms of granules or by
79 binding to molecules such as metallothioneins (MTs) or metallothionein-like proteins in cytosols
80 (Wallace et al., 2003; Vijver et al., 2004).

81 Therefore, to obtain the insight into biomolecules targeted by the metals and affected
82 metabolic and physiological pathways, new approach, called metallomics, was developed
83 (Szpunar, 2004). Combination of size-exclusion liquid chromatography (SEC-HPLC) and
84 inductively coupled plasma mass spectrometry (ICP-MS) is one of recognized approaches for

85 screening cytosolic metal distribution among biomolecules of different molecular sizes. This
86 methodology has already been used for determination of the cytosolic metal distribution in
87 different tissues of aquatic organisms including bivalves *Mytilus galloprovincialis* (Strižak et al.,
88 2014) and *Perna perna* (Lavradas et al., 2016), or fish such as European eel (*Anguilla anguilla*;
89 Goenaga Infante et al., 2003), yellow perch (*Perca flavescens*; Caron et al., 2018), white sucker
90 (*Catostomus commersonii*; Urien et al., 2018), European and Vardar chub (*Squalius cephalus*
91 and *Squalius vardarensis*; Krasnići et al., 2013, 2014, 2018, 2019), brown trout (*Salmo trutta*;
92 Dragun et al., 2018b) and Prussian carp (*Carassius gibelio*; Dragun et al., 2020).

93 As a continuation of comprehensive study of anthropogenic impact on Croatian rivers,
94 Krka and Ilova, we have, for the first time, chosen the intestine of brown trout and Prussian carp,
95 for the analysis of molecular masses (MM) of cytosolic biomolecules that bind specific trace
96 elements. Both of the investigated rivers are under moderate influence of industrial and
97 municipal wastewaters (Filipović Marijić et al., 2018; Sertić Perić et al., 2018; Mijošek et al.,
98 2020). So far, we have investigated seasonal and spatial variability of total and cytosolic metal
99 levels, as well as biomarker responses in the intestine of these two fish species (Mijošek et al.,
100 2019a, 2019b, 2021). Although there are few studies dealing with sub-cellular partitioning of
101 metals in the fish intestine (Oyo-Okooth et al., 2012; Filipović Marijić and Raspor, 2014), to the
102 best of our knowledge there is no available data on distribution of any element among cytosolic
103 molecules of different molecular masses in the intestine of any fish species. Despite its great
104 importance in fish digestion and dietborne metal uptake (Clearwater et al., 2000), intestine is still
105 rarely used as a bioindicator tissue.

106 Thus, we applied SEC-HPLC combined with offline metal measurement using high
107 resolution ICP-MS (HR ICP-MS) to separate, for the first time, intestinal cytosols of two fish

108 species into fractions with the main aim to define the distribution among biomolecules of
109 different MM for seven selected elements, including nonessential Cd and six essential elements
110 (Co, Cu, Fe, Mo, Se, and Zn). The additional aim was to establish the differences/similarities
111 between two studied species, as well as the differences/similarities between intestinal
112 metal/nonmetal distributions and distributions reported for the other organs of the same fish
113 species (Dragun et al., 2018b; Dragun et al., 2020). Moreover, the goals of the study were also
114 to detect possible differences in metal-handling strategies of fish dwelling in differently polluted
115 areas and of fish caught during the spawning (autumn) and post-spawning period (spring).

116

117 **2. Materials and methods**

118 2.1. Study areas

119 Two areas of differing ecological characteristics were selected, the karst Krka River and
120 lowland Ilova River. Krka River is Dinaric karst river in the coastal region of southern Croatia
121 which catchment area covers about 2500 km², while its length is about 73 km. An average annual
122 discharge is 47.4 m³ s⁻¹ (1990-2009) (Čanjevac and Orešić, 2015). Due to the tuffa barriers and
123 waterfalls and high biodiversity, considerable part of the river was proclaimed national park in
124 1985. The Ilova River is a Pannonian river in the continental part of central Croatia with a total
125 catchment area of about 1128 km², length of about 96 km and average annual discharge of 7.3
126 m³ s⁻¹ (Čanjevac and Orešić, 2015). The lower part of its watercourse is a part of the Lonjsko
127 Polje Nature Park.

128 At both watercourses, samplings involved two sampling sites of different pollution impact
129 (reference and contaminated) and two sampling campaigns covering different physiological
130 conditions of fish, specifically spawning (autumn) and post-spawning period (spring). The

131 concentrations of elements investigated in this study at all sampling sites in two seasons are
132 given in Table 1 (Sertić Perić et al., 2018; Mijošek et al., 2020).

133 At Krka River, sampling campaigns were conducted in October 2015 and May 2016. As a
134 reference site, river source was selected, whereas contaminated site was located downstream of
135 the Town of Knin, due to the known pollution sources (industrial wastewaters of screw factory
136 and untreated municipal wastewaters of the Town of Knin). The information on sampling sites
137 and water quality were already published (Filipović Marijić et al., 2018; Sertić Perić et al., 2018),
138 as well as on metal accumulation in fish intestine (Mijošek et al., 2019a, 2019b). Generally,
139 dissolved metals in water with the highest concentrations at contaminated site were Fe, Li, Mo,
140 Sr, Rb and Ca, while physico-chemical water parameters (temperature, conductivity, nitrates,
141 total dissolved solids and water hardness) supported the findings on slightly deteriorated
142 environmental conditions near the Town of Knin (Sertić Perić et al., 2018). Of elements analyzed
143 in this study, Fe and Mo were considerably higher in water from the contaminated site (Town of
144 Knin), while Cu and Zn were below LOD at all sites and seasons (Table 1).

145 At Ilova River, the samplings were conducted in October 2017 and May 2018. The
146 reference site was located upstream of contamination sources near the Ilova village, while
147 contaminated site, affected by municipal (the Town of Kutina) and industrial (fertilizer factory)
148 wastewaters, was located near the Trebež village. The information on sampling sites and water
149 and sediment quality were already published (Mijošek et al., 2020), as well as on metal
150 accumulation in the intestine of Prussian carp (Mijošek et al., 2021). Mijošek et al. (2020a)
151 reported that many elements were significantly elevated in water and sediments from the Trebež
152 village compared with the Ilova village. Arsenic, Cd, Cu, Ni, Pb and V were among the elements
153 of highest concern due to the highest differences between the sites. Additionally, as in the Krka

154 River, physico-chemical parameters including total dissolved solids, nitrates and phosphates
155 confirmed lower water quality at the contaminated site of the Ilova River. Among analyzed
156 elements, Cd, Mo and Se in both seasons, and Co and Fe in one season were elevated in the
157 water samples from contaminated site (Trebež village) (Table 1). All elements except Zn were
158 higher in the Ilova than Krka River so fish from the Ilova River were exposed to higher water
159 metal concentrations indicating that some specific differences in metal handling strategies and
160 defense mechanisms of the two fish species might be presumed.

161

162 2.2. Fish sampling and tissue dissection and preparation

163 The selected bioindicator organisms were representative native fish from the Krka and
164 Ilova rivers, brown trout (*Salmo trutta* Linnaeus, 1758) and Prussian carp (*Carassius gibelio*
165 Bloch, 1782), respectively. Sampling campaigns were performed by electro-fishing, following
166 the Croatian standard HRN EN 14011. Fish were kept alive in an opaque plastic tank filled with
167 aerated river-water. Among the sampled fish, we selected twelve specimens from each
168 ecosystem for cytosolic metal distribution analyses, three per each site in each season. Basic
169 biometric characteristics of used fish are presented in Table 2. In the laboratory, fish were
170 anesthetized using tricaine methane sulphonate (MS 222, Sigma Aldrich) in accordance with the
171 Ordinance on the protection of animals used for scientific purposes (NN 55, 2013). Fish total
172 body mass and total lengths were recorded and sex determined. Digestive tract was removed on
173 ice and intestinal part was cut off and cleaned of exterior fat, gut content and intestinal fish
174 parasites, acanthocephalans. Finally, intestinal tissue was rinsed with MQ water, weighed and
175 frozen immediately in liquid nitrogen in cryogenic polypropylene containers until their transfer
176 to $-80\text{ }^{\circ}\text{C}$ and further analyses.

177

178 2.3. Homogenization procedure and preparation of intestinal cytosolic fractions

179 Homogenization procedure of the fish intestinal tissue has been described in detail by
180 Mijošek et al. (2019a). Homogenization buffer contained 100 mmol L⁻¹ Tris-HCl/base (Merck,
181 Germany, pH 8.1 at 4 °C), 1 mmol L⁻¹ DTT (Sigma, USA) as a reducing agent, 0.5 mmol L⁻¹
182 PMSF (Sigma, USA) and 0.006 mmol L⁻¹ leupeptin (Sigma) as protease inhibitors. Intestinal
183 tissue was homogenised on ice in five volumes of buffer at 6000 rpm by Potter-Elvehjem
184 homogenizer (Glas-Col, USA). Obtained homogenates were afterwards centrifuged by Avanti J-
185 E centrifuge (Beckman Coulter, USA) at 50,000×g for 2 h at 4 °C, and the resulting supernatant
186 corresponded to total soluble cytosolic fraction, which was stored at -80 °C.

187

188 2.4. SEC-HPLC fractionation of intestinal cytosols of brown trout and Prussian carp

189 The distributions of elements among biomolecules of different MM in the cytosols of the
190 intestine of brown trout and Prussian carp were determined using HPLC system (Perkin Elmer,
191 200 series, USA). Tricorn Superdex TM 200 10/300 GL column with a separation range of 10–
192 600 kDa (GE Healthcare Biosciences, USA) was used as described by Krasnići et al. (2013,
193 2014, 2018, 2019) and Dragun et al. (2018b, 2020). 20 mmol L⁻¹ Tris-HCl/Base buffer solution
194 (Sigma–Aldrich, pH 8.1 at 22 °C) was used as the mobile phase at a flow rate of 0.5 mL min⁻¹
195 (isocratic mode). The supernatant (cytosol) samples were injected directly into the HPLC system.
196 One-minute fractions were collected starting at 13th minute and ending at 52nd using a fraction
197 collector (Gilson FC 203B) after two consecutive injections (100 µL of supernatant sample each)
198 and two chromatographic runs. For column calibration, seven protein standards (thyroglobulin,
199 apoferritin, b-amylase, alcohol dehydrogenase, bovine albumin, and carbonic anhydrase, Sigma,

200 USA) diluted in 20 mmol L⁻¹ Tris-HCl/Base buffer solution were run through the column under
201 the same conditions as the samples and obtained equation of the calibration straight line is given
202 in Table 3. Calibration straight line was created based on known MM of protein standards and
203 their respective elution times (t_e ; Table 3). Metallothionein (MT) standards (Enzo
204 Metallothionein-1, Enzo Metallothionein-2, Enzo Life Sciences, Switzerland) were also run
205 through the column, whereas the void volume (V_o) of the column was determined by use of blue
206 dextran.

207

208 2.5. Measurement of trace element concentrations in the SEC-HPLC fractions of intestinal 209 cytosols

210 Cytosolic trace element concentrations in the intestinal tissue of brown trout and Prussian
211 carp were previously measured and reported by Mijošek et al. (2019b, 2021), and are now given
212 in Table 2 for seven elements analyzed in this study. In present study, we have measured
213 concentrations in one-minute fractions obtained by SEC-HPLC separation of cytosols. Fractions
214 collected after SEC-HPLC separation were only acidified with HNO₃ (Suprapur, Merck,
215 Germany, final acid concentration in the samples: 0.16%) prior to measurements. Indium (Fluka,
216 Germany) was added to all samples as an internal standard (1 µg L⁻¹). High resolution
217 inductively coupled plasma mass spectrometer (HR ICP-MS, Element 2, Thermo Finnigan,
218 Germany), equipped with an autosampler SC-2 DX FAST (Elemental Scientific, USA) was used
219 for the measurements. Measurements of ⁸²Se, ⁹⁸Mo and ¹¹¹Cd we performed in low resolution
220 mode, whereas ⁵⁶Fe, ⁵⁹Co, ⁶³Cu, and ⁶⁶Zn in medium resolution mode. External calibration was
221 performed using diluted multielement standard solution for trace elements (Analitika, Czech
222 Republic), prepared in 1.3% HNO₃ (Suprapur; Merck, Germany), supplemented with In (1 µg

223 L⁻¹; Fluka, Germany). Limits of detection (LODs) were reported by Krasnići et al. (2018) and
224 Dragun et al. (2018b, 2020). The accuracy of measurements was checked by analysis of quality
225 control sample (QC for trace metals, catalog no. 8072, lot no. 146142-146143, Burlington,
226 Canada) and the following recoveries (%) were obtained based on 13 measurements: Cd
227 96.2±1.8; Co 96.8±1.7; Cu 97.3±1.3; Fe 96.9±4.4; Mo 97.4±2.4; Se 96.7±5.8; and Zn
228 106.6±13.7.

229

230 2.6. Data processing and statistics

231 Microsoft Excel 2007 and SigmaPlot 11.0 for Windows were used for data processing and
232 creation of graphs. Column calibration (Table 2) enabled association of elution times of specific
233 peaks to corresponding MM, with the aim to define MM of biomolecules that bind each element
234 (Table 4). Based on t_e of protein standards and the chromatographic profiles of metals and
235 previous studies (Krasnići et al., 2013, 2018), biomolecules were categorized in four classes: a
236 high molecular mass range (HMM; >100 kDa), a medium molecular mass range (MMM; 30-
237 100 kDa), a low molecular mass range (LMM; 10-30 kDa) and a very low molecular mass range
238 (VLMM; <10 kDa).

239

240 **3. Results and discussion**

241 3.1. Fish biometry and cytosolic metal concentrations

242 The information on cytosolic intestinal metal levels in the same fish as analyzed in this
243 study was previously published as a part of comprehensive research of metal exposure and
244 bioaccumulation in brown trout and Prussian carp (Mijošek et al., 2019b; 2021). In the presented

245 research, element distribution among biomolecules was assessed at different bioaccumulation
246 rates by choosing fish individuals with variable cytosolic metal concentrations.

247 Biometric characteristics of twelve selected specimens of each species, as well as their
248 cytosolic metal levels are listed in Table 2. Brown trouts used in this research were 16.2-27.8 cm
249 long and had masses of 46.7-201.7 g. Altogether, we have analyzed five females and seven
250 males (Table 2). Prussian carps varied in total length from 17.1 to 27.2 cm and weighed from
251 83.36 to 339.19 g. Female predominance was evident, as already noted by few authors for
252 Prussian carp (Erdogan et al., 2014; Dragun et al., 2020), with eight females and four males
253 analyzed (Table 2). However, comparison of obtained element distribution profiles did not
254 indicate any considerable variations regarding fish sex or size. Differences, mainly referring to
255 peak heights, were mostly the consequence of variable intestinal accumulation in investigated
256 specimens.

257

258 3.2. Distribution of trace elements in the intestinal cytosols of brown trout and Prussian carp

259 Distribution profiles of seven analyzed elements among cytosolic biomolecules of different
260 MM in the intestine of brown trout and Prussian carp are presented in Figs. 1-4 for each river and
261 location, while their elution times and MM of corresponding biomolecules are given in Table 4.
262 Sampling season is also indicated in figures to consider the differences that might occur due to
263 the physiological variability and reproductive status of fish species. In general, specific seasonal
264 and spatial trends were mostly not observed in presented research, but rather connection with
265 different levels of bioaccumulation. Each investigated element will further be independently
266 presented and discussed.

267

268 3.2.1. Cadmium

269 Cd is considered as nonessential and toxic element, and it was distributed within a single
270 peak in LMM biomolecule region (28th-38th minute) in the majority of specimens of both
271 investigated fish species (Fig. 1a-d). The peaks maxima were at 30th-32nd minute, which
272 corresponded to biomolecules of MM of 11-18 kDa (Table 4) and the elution time of two MT-
273 standards (Table 3). The mass of 11-18 kDa could at first point to presence of MT dimers in fish
274 intestine, which is a form often found in different fish species at MM of 10-15 kDa (Kito et al.,
275 1982; Chatterjee and Maiti, 1987; Kammann et al., 1996; Hauser Davis et al., 2012). However,
276 previous study on Vardar chub liver and gills, indicated that SEC-HPLC technique overestimates
277 the molecular masses of small proteins; thus, the MM of MTs, which was estimated at 15 kDa by
278 SEC-HPLC, was further on confirmed to be 6 kDa using MALDI-TOF MS (Krasnići et al.,
279 2019). Only small portion, almost negligible, of Vardar chub hepatic MT was present in the form
280 of dimer (Krasnići et al., 2019). Our finding confirmed the well-known affinity of MTs for Cd
281 binding, as one of the most important mechanisms for its detoxification (Roesijadi et al., 1992;
282 McGeer et al., 2012). Obtained profiles, which differences referred only to the increase of peak
283 height following the increase of cytosolic Cd concentrations, without specific spatial and
284 seasonal patterns, suggested high detoxification rate of Cd when present in low and moderate
285 concentrations. Due to the mostly higher concentrations of Cd in autumn compared with spring
286 at all locations, peak heights were generally higher in autumn (Fig. 1a), but additional peaks did
287 not occur. However, slight association of Cd with HMM region was observed in samples with
288 highest cytosolic concentrations (in Prussian carp from Trebež village), indicating possible
289 higher susceptibility to Cd toxicity after its higher bioaccumulation. Generally, the presumable
290 Cd-MT peaks were higher in the Prussian carp than brown trout, probably owing to considerably

291 higher intestinal Cd cytosolic concentrations in that fish (Fig. 1a-d, Table 2). Dominant binding
292 of Cd to MTs has already been described in the liver of brown trout (Dragun et al., 2018b) and
293 liver and gills of Prussian carp (Dragun et al., 2020) from the same samplings. Comparison of
294 intestinal Cd distribution with the distributions in the other two organs from these species
295 revealed variability only in heights of the existing peaks, as a consequence of different cytosolic
296 Cd concentrations (Dragun et al., 2018b, 2020). Probable binding of Cd to MTs was also
297 observed in the liver of variety of fish species (Goenaga Infante et al., 2003; van Campenhout et
298 al., 2010; Krasnići et al., 2013, 2018; Urien et al., 2018), indicating dominant Cd detoxification
299 by MTs.

300

301 3.2.2. Copper

302 Copper is an essential element known to have an important role in fish metabolic processes
303 involving its catalytic and structural function in various enzymes and metalloproteins (Festa and
304 Thiele, 2011). Although the dominant LMM peak was almost the same as in the case of Cd
305 (maxima at 11-18 kDa; Table 4) indicating predominant Cu binding to MT, there was an
306 additional peak in MMM biomolecules range of both fish species (Fig. 1e-h) at elution times
307 from 24th to 30th minute (biomolecules MM range from 18 to 85 kDa). That peak has
308 encompassed many other proteins known to contain Cu, such as albumin (66 kDa), superoxide
309 dismutase (32 kDa) and carbonic anhydrase (29 kDa) (Szpunar and Lobinski, 1999; Table 3), but
310 it was much less pronounced in all cases than presumable Cu-MT-peak (Fig. 1e-h). Specific
311 seasonal and spatial patterns were generally not observed, with the exception of peaks in brown
312 trout from the Krka River source which, due to the lowest cytosolic Cu concentrations, were not
313 so clear and defined as in the fish from the other sites, but still revealed the similar distribution

314 patterns (Fig. 1e). At the site near the Town of Knin, higher Cu peak heights were observed in
315 autumn, probably due to higher concentrations of many essential elements in spawning periods
316 of fish, which is autumn for brown trout. Variability of Cu distribution mainly referred to
317 increase of peak height and area of Cu LMM-peak following the increasing Cu cytosolic
318 concentrations (Fig. 1e-h, Table 2), with peak widening which possibly indicated Cu association
319 to the other cytosolic biomolecules when present in the cell in higher concentrations. In the liver
320 of brown trout the predominant binding of Cu to LMM region was also previously confirmed,
321 suggesting the crucial role of MTs, but additional peaks in HMM biomolecule range were also
322 observed when Cu was present in higher cytosolic concentrations (Dragun et al., 2018b). An
323 indication of such peaks was also visible in the brown trout intestine at elution time from 13th to
324 17th minute in the samples with higher Cu intestinal concentrations (Fig. 1e, f). Comparison of
325 Cu distribution in the intestine of Prussian carp with liver and gills of the same species indicated
326 that intestinal Cu distribution was more similar to liver than to gills, with majority of Cu eluted
327 in LMM region (Dragun et al., 2020). Generally, many studies confirmed dominant Cu elution at
328 the elution time of MTs in many other fish species and tissues (van Campenhout et al., 2008;
329 Krasnići et al., 2013, 2014, 2018; Caron et al., 2018; Urien et al., 2018).

330

331 3.2.3. Cobalt

332 Cobalt distribution included four separate Co-containing peaks in both fish species (Fig.
333 2a-d, Table 4), but there were differences in predominant peaks between the species. In brown
334 trout, predominant binding of Co to HMM molecules was observed (85-235 kDa). This finding
335 was consistent with Co distribution in hepatic cytosol of brown trout from the Krka River where
336 even higher increase of Co quantity was observed in the HMM peak (Dragun et al., 2018b),

337 similar as in the liver and gills of European and Vardar chub (Krasnići et al., 2013, 2014, 2018),
338 and liver of juvenile yellow perch (Caron et al., 2018). Only smaller part of Co in brown trout
339 intestine binded to MMM (30-85 kDa) or VLMM (0.5-18 kDa) biomolecules (Fig. 2a,b). The
340 MMM-peak included the elution time of the bovine albumin standard (Table 3), known to have a
341 role in binding and transport of metals, including Co (Sadler et al., 1994). Two less clear peaks,
342 especially in samples with the lowest Co cytosolic concentrations, corresponded to VLMM
343 biomolecules region (elution times from 30th to 38th minute, and from 39th to 44th minute; Table
344 4). The opposite trend was revealed in Prussian carp from the Ilova River, where similar
345 distribution occurred, but predominant binding to VLMM biomolecules was observed at both
346 investigated sites (Fig. 2c, d). The first VLMM-peak was higher and corresponded to molecules
347 of 2.4-18 kDa. The other smaller VLMM-peak corresponded to biomolecules of 0.7-1.8 kDa
348 (Table 4), and included MM of cobalamine (vitamin B12, 1.3 kDa; Kirschbaum, 1981),
349 confirming the role of essential Co in building cobalamine structure (Blust, 2012). Although this
350 possible link with cobalamine was more pronounced in Prussian carp, it was also observed in the
351 intestine of brown trout, contrary to the liver of brown trout where this peak was not clearly
352 visible (Dragun et al., 2018b). In Prussian carp, almost negligible portion of Co was associated
353 with HMM and MMM regions (Fig. 2c, d). The significant impact of season or site on the
354 obtained profiles was not noticed except in the Krka River source where peak heights were
355 always higher in autumn than spring (Fig. 2a). The increase of Co quantity in HMM region was
356 observed due to the increasing cytosolic Co concentrations (Fig. 2a-d). The highest cytosolic
357 concentration and peak heights observed in brown trout from the Town of Knin (Fig. 2b). In
358 Prussian carp, the differences between the peaks were not that pronounced, and only slightly

359 increased Co elution in VLMM region was observed with higher Co bioaccumulation (Fig. 2c,
360 d).

361

362 3.2.4. Iron

363 As essential element, Fe has important physiological roles in oxygen transport as integral
364 part of hemoglobin or as a part of enzyme cytochrome c oxidase, which participates in
365 mitochondrial respiratory chain (Bury et al., 2012). Further, it is involved in DNA synthesis and
366 metabolism of collagen, fatty acids or tyrosine (Kuhn et al., 2016), as well as in protection
367 against bacterial infections (Vidal et al., 1993). Iron distribution profiles indicated its presence in
368 two or three areas of MM, depending on the fish species. The first peak in the HMM area (182-
369 1088 kDa) and the second one in the MMM area (18-109 kDa) were common for both fish
370 species (Table 4). Maximum of the HMM peak was associated to biomolecules of 400-500 kDa
371 and likely presented binding to ferritin (450 kDa; Szpunar and Lobinski, 1999), Fe storage
372 protein, whereas MMM peak covered MM of several Fe-containing biomolecules, such as blood
373 protein hemoglobin (65 kDa) or its subunits (Krasnići et al., 2019), transport proteins transferrin
374 (80 kDa; Asmamaw, 2016) and ferroportin (63 kDa), or enzyme catalase subunits (each of 60
375 kDa) (Martin-Antonio et al., 2009). Dominant peak in brown trout was observed in MMM
376 biomolecule range (Fig. 2e, f), whereas the first peak in HMM region was dominant in Prussian
377 carp (Fig. 2g, h). The clear third peak was observed only in brown trout in the LMM/VLMM
378 range, covering an area of 1.8–14 kDa (Fig. 2e, f), which suggested possible binding to
379 nucleotides, amino acids, pyrophosphates, and Fe complexes (Beard et al., 1996). In Prussian
380 carps, there was no peak in VLMM biomolecule range, but a slight indication of a peak in LMM
381 biomolecule region (5.1-14 kDa) was visible in a few samples (Fig. 2g, h). Intestinal Fe

382 distribution in brown trout was comparable with hepatic distribution in the same species, with
383 three peaks observed (Dragun et al., 2018b). Only difference was that in hepatic samples HMM
384 peak was dominant, probably due to higher Fe concentrations in liver than intestine, suggesting
385 more important role of the liver in Fe storage (Walker and Fromm, 1976; Dragun et al., 2018b).
386 In Prussian carp, two peaks observed in the intestine were also observed in the liver and gills,
387 where MMM peak was shown to be predominant in the gills and HMM peak in liver, similar to
388 the intestine (Dragun et al., 2020). We further observed similarity of intestinal Fe distributions of
389 Prussian carp with hepatic and gill distributions in European and Vardar chub, where binding of
390 Fe in VLMM region was also not observed (Krasnići et al., 2013, 2014, 2018) suggesting some
391 similar mechanisms of Fe binding in species belonging to the same fish family (Cyprinidae).
392 Specific seasonal and spatial trends were not observed, but connection with different levels of
393 bioaccumulation. In both fish species, elevated Fe concentrations were accompanied by an
394 increase in the HMM or MMM peak, depending on the specimen.

395

396 3.2.5. Molybdenum

397 Molybdenum serves as a cofactor in various enzymes including Fe-Mo flavoprotein
398 xanthine oxidase (275 kDa, Truglio et al., 2002), aldehyde oxidase (130 kDa, Uchida et al.,
399 2003) or sulfite oxidase (120 kDa; Johnson and Rajagopalan, 1976). Its distribution was similar
400 in the intestine of both investigated fish species with two well shaped and clear peaks in HMM
401 (~100-400 kDa, Table 4) and VLMM (~2-8 kDa, Table 4) biomolecule range, and the VLMM
402 peak was visibly predominant in both species (Fig. 3a-d). Generally, Mo cytosolic concentrations
403 were higher in Prussian carp than in brown trout which affected peak heights and quantity of
404 eluted Mo (Fig. 3a-d, Table 2). Although MMs of all above mentioned enzymes were

405 encompassed by the observed HMM peak, this peak was much smaller compared to VLMM
406 peak, suggesting less significant Mo binding to enzymes in the intestine. For comparison, HMM
407 peak was dominant and much more pronounced than VLMM peak in the liver of both brown
408 trout and Prussian carp (Dragun et al., 2018b, 2020), as well as of European and Vardar chub
409 (Krasnići et al., 2013, 2018), confirming the organ-specificity of these enzymes that have
410 important roles in detoxification of xenobiotics, drugs and progesterone (Kisker et al., 1997),
411 which mostly takes place in the liver as main detoxifying and metabolic organ (van Campenhout
412 et al., 2008). The dominant peak in our research, in the intestine of both Prussian carp and brown
413 trout, was located in VLMM region (maximum at 5.1 kDa; Fig. 3a-d, Table 4), same as observed
414 in the gills of Prussian carp (Dragun et al., 2020), suggesting higher similarity in function of
415 intestine with gills as uptake organs, than with the liver. Krasnići et al. (2019) have shown that
416 VLMM Mo-binding biomolecules were heat-stable and determined their exact mass to be 3.3
417 kDa, which corresponded well to the estimated MM of predominant Mo-binding biomolecules in
418 the intestine of brown trout and Prussian carp. The significant impact of season or site on the
419 obtained profiles was not noticed and in both species, the increase of Mo elution in samples with
420 higher cytosolic concentrations was seen in both peaks, but it was much more pronounced in the
421 second, VLMM peak (Fig. 3a-d). Evidently, variability in different organs of the same species
422 can be attributed to their different bioaccumulation capacities and different role of Mo in each
423 organ. Presence in the intestine as a site of dietborne metal uptake, and gills as the site of
424 waterborne metal uptake probably reflect recent Mo uptake and indicate binding to small
425 metallochaperons or nonprotein compounds (Dragun et al., 2020).

426

427 3.2.6. Selenium

428 Selenium biological role is primarily related to incorporation into proteins in a form of
429 selenocysteine, and is found, for example, in glutathione peroxidase, thioredoxin reductase and
430 vitamin E (Watanabe et al., 1997). We noticed several species-specific differences in Se
431 distribution in our research which included differences in number of peaks and peak
432 predominance between the two species (Fig. 3e-h, Table 4). Distribution profiles of Se in the
433 intestine of the brown trout showed its predominant presence within two peaks in VLMM range,
434 one covering biomolecular region from 1.8-5.1 kDa (maximum at 3.9 kDa) and another one
435 covering biomolecules of less than 1.5 kDa (Fig. 3e, f, Table 4). This second peak was
436 predominant at both locations of the Krka River (Fig. 3e, f). In some brown trout specimens, two
437 barely visible peaks were also observed in HMM region (500-100 kDa and 65-235 kDa; Fig. 3e,
438 f). In the liver of brown trout, Se association with biomolecules below 1.5 kDa was also the most
439 pronounced (Dragun et al., 2018b). Major binding of Se to biomolecules below 2 kDa was
440 already reported in gills of European and Vardar chub (Krasnići et al., 2014, 2018), but not in the
441 liver (Krasnići et al., 2013, 2018). Such Se elution in VLMM region could refer to forms of free
442 selenocysteine (167 Da) or selenomethionine (196 Da) in the cytosols, as fish mostly accumulate
443 Se in these forms and gastrointestinal uptake is central to both nutritional Se requirements and its
444 toxicity (Janz et al., 2010). Further, it may indicate binding to compounds active in defense
445 against oxidative stress, such as selenoneine (0.5 kDa, Yamashita and Yamashita, 2010). In
446 addition to two VLMM peaks, which in Prussian carp encompassed biomolecules of 0.4–11 kDa,
447 possibly including low MM selenoprotein SelW (~10 kDa), protein that possibly participates in
448 antioxidant function (Lopez Heras et al., 2011), in this species Se was also comparably eluted in
449 HMM region (30-303 kDa; maximum at 110 kDa; Fig. 3g, h). This HMM range includes known
450 selenoproteins, such as glutathione peroxidase (85 kDa, Shulgin et al., 2008) or thioredoxin

451 reductase (66 kDa), as well as selenoprotein SelP (50 kDa) identified in zebra fish (*Danio rerio*),
452 primarily synthesized in liver and involved in the transport and delivery of Se to remote tissues
453 (Kryukov and Gladyshev, 2000). As in brown trout, in some samples of Prussian carp additional
454 small HMM peak was indicated at elution time from 14th to 18th minute (Fig. 3g, h). In Prussian
455 carp, the increase in Se accumulation at the Ilova village was mainly reflected in its increased
456 presence in the HMM biomolecule region, while at Trebež village higher amount of Se was
457 bounded to VLMM biomolecules (Fig. 3g, h), regardless of the fact that Se in the intestine
458 cytosol was present in a relatively narrow concentration range in fish from both locations of the
459 Ilova River (Table 2). In brown trout, the increase in intestinal cytosolic Se concentrations was
460 not site-specific and resulted in a more pronounced presence in the VLMM biomolecule region,
461 precisely in the second VLMM peak (<2 kDa) at both sites. Similarly to Co and Cu, Se
462 concentrations were higher in the spawning period of brown trouts which resulted in higher
463 peaks in autumn than spring at both locations of the Krka River (Fig. 3a, b). Previous research on
464 Prussian carp showed the existence of four peaks in gills with major part of Se being eluted in
465 two VLMM peaks, whereas in the liver majority of Se was eluted within one HMM peak and
466 only minor part was eluted within two VLMM peaks (Dragun et al., 2020). Therefore, the
467 intestinal distribution profiles of Se in Prussian carp unite the characteristics of both gills and
468 liver, with observed Se elution being almost comparable in HMM and VLMM regions (Fig. 3g,
469 h). Recorded species-specific differences between brown trout and Prussian carp could be
470 associated to the variability of their feeding behavior (Maher, 1987), and to differences in Se
471 metabolism between the species.

472

473 3.2.7. Zinc

474 Zinc essentiality is reflected by its role in metabolism of different biomolecules including
475 proteins, carbohydrates and lipids, but also in cell signalization, protection of the immune system
476 and neurotransmission, therefore encompassing catalytic, regulatory, and structural functions
477 (Coelman, 1992). Therefore, its distribution in relatively wide range of MM was not unexpected.
478 Moreover, species-specific differences between brown trout and Prussian carp were observed
479 (Fig. 4). In brown trout, Zn was eluted in two clear peaks in HMM biomolecule region. First and
480 dominant peak covered the biomolecules of 392-1088 kDa, and the second one of 30-235 kDa,
481 with the maxima at ~600-800 kDa and 85-109 kDa, respectively (Table 4). This range could
482 suggest binding to different proteins such as albumin (66 kDa, Table 3) or transferrin (80 kDa),
483 carbonic anhydrase (29 kDa, Table 3), Zn superoxide dismutase (32 kDa, Table 2) and alcohol
484 dehydrogenase (150 kDa, Table 3). Similar distribution, with the predominant peak at 20-400
485 kDa which corresponded well to our second HMM peak, but with the additional LMM peak (9-
486 19 kDa), which coincided with the elution time of MT standard, was observed in the hepatic
487 cytosols of brown trout (Dragun et al., 2018b). In Prussian carp, in addition to above mentioned
488 two HMM peaks (maxima at 843 kDa and 109 kDa, respectively), elution in VLMM region was
489 also observed (Fig. 4c, d, Table 4). Although Zn in VLMM region was eluted in broad range, by
490 careful insight two separate peaks could be distinguished in most samples (Fig. 4c, d), the first at
491 1.8-14 kDa, and the second one at 0.7-1.8 kDa, and the predominant binding to VLMM was
492 mostly observed for specimens with the higher Zn intestinal cytosolic concentrations (Fig. 4c, d).
493 Therefore, in Prussian carp there was an indication of possible binding to MT (the tail of the first
494 VLMM peak), but this was not clear and pronounced. More dominant Zn association with MT
495 region was observed in liver of Prussian carp, while hepatic Zn HMM peaks appeared at MMs of
496 30–300 kDa and above 400 kDa (Dragun et al., 2020) comparable to intestine. The significant

497 impact of season or site was not noticed. Intestine was, as in the case of some other elements,
498 confirmed to be more similar to gills as the uptake tissue, in which clear binding to MTs was also
499 not observed in Prussian carp, but neither in European nor Vardar chub (Krasnići et al., 2014,
500 2018; Dragun et al., 2020). In addition, two VLMM peaks were also observed in both the gills
501 and the liver of Prussian carp (Dragun et al., 2020), as well as of European chub (<5 kDa),
502 especially in the specimens with higher cytosolic Zn concentrations (Krasnići et al., 2013).
503 Elution in VLMM biomolecule range could indicate role of Zn in antioxidative defense by
504 binding to glutathione (GSH, 307 Da, <https://pubchem.ncbi.nlm.nih.gov/compound/Glutathione>),
505 intracellular thiol compound composed of cysteine, glutamic acid and glycine, which can be free
506 in the cells or bound to proteins (Iwasaki et al., 2009). This mechanism of detoxification by GSH
507 might occur in the fish intestine, as GSH quantity was shown as quite high in the intestine of
508 brown trout and Prussian carp (Mijošek et al., 2019a, 2021). Zinc distribution profiles slightly
509 differed for different species or different tissues, due to differences in biology and ecology of the
510 species, their different accumulation and detoxification mechanisms, as well as tissue
511 composition or specific role.

512

513 **4. Conclusions**

514 Applied methodology enabled us to define, for the first time, the molecular mass ranges of
515 cytosolic molecules that bind Cd, Co, Cu, Fe, Mo, Se and Zn in the intestines of brown trout and
516 Prussian carp from two moderately contaminated rivers. Although we considered spatial and
517 temporal variability at each river, comparison of the obtained profiles indicated that distribution
518 of trace elements among different biomolecules was mostly dependent on level of exposure and
519 consequent bioaccumulation. Significant differences associated to seasons were not observed,

520 and trace elements under all studied conditions were associated to the same biomolecules, and
521 only the proportions associated to specific cytosolic compounds changed as a consequence of
522 different concentrations of elements. Well-established link of Cd and Cu to MTs was confirmed
523 for the intestine of both fish species, suggesting efficient detoxification of these elements, as well
524 as functional association in case of Cu. However, association of Zn to MTs was not observed in
525 the intestine, contrary to previously established presence of Zn-MT binding in the liver of brown
526 trout and Prussian carp. Further, Fe, Se and Zn showed some considerable species-specific
527 differences in our research. Specifically, Fe elution in VLMM biomolecule range was observed
528 only in brown trout, while Se was eluted in HMM and Zn in VLMM biomolecule range only in
529 Prussian carp. Additionally, Co was found to predominantly bind to biomolecules of MM of 85-
530 235 kDa in brown trout, but to biomolecules of MM <18 kDa in Prussian carp, but the same
531 peaks were observed in both species. Tissue-specific differences were additionally observed for
532 Fe, Se and Zn distribution between intestinal, hepatic and gills cytosols. They reflected different
533 functions of these organs, showing some similarities of the intestine with both gills and liver, but
534 more clear with gills, as both being the uptake organs. Comparison with other fish species also
535 indicated species-specific variability, due to the different ecology of the species, their
536 accumulation capacities and specific metal handling strategies. As there is no available data on
537 metal-binding biomolecules in the fish intestine, the results obtained within this study present a
538 significant contribution to better understanding of the fate of those elements, their detoxification
539 mechanisms and behavior in fish intestinal tissue, specifically in brown trout and Prussian carp.
540 Comparison with the literature data for the other organs suggested the importance of studying
541 intracellular metal distribution in various tissues, as their primary role has significant impact on
542 metal handling strategies. The information presented here can serve as a basis for future research,

543 involving additional separation methods and mass spectrometry techniques for accurate
544 identification of the exact metal binding molecules, which could enable the clarification of metal
545 toxicity and detoxification mechanisms.

546

547 **5. Acknowledgements**

548 The study was conducted within the project “Accumulation, subcellular mapping and effects of
549 trace metals in aquatic organisms” (project no.: IP-2014-09-4255), financed by Croatian Science
550 Foundation. Authors are thankful for assistance in fish sampling to colleagues from Laboratory
551 for Aquaculture and Pathology of Aquatic Organisms from the Ruđer Bošković Institute.

552

553 **6. References**

554 Asmamaw, B., 2016. Transferrin in fishes: A review article. *J. Coast. Life Med.* 4, 176-180.

555 Beard, J.L., Dawson, H., Pifiero, D.J., 1996. Iron metabolism: a comprehensive review. *Nutr.*
556 *Rev.* 54, 295–317.

557 Blust, R., 2012. Cobalt. In: Wood, C.M., Farrell, A.P., Brauner, C.J. (Eds.), *Fish Physiology:*
558 *homeostasis and toxicology of essential metals.* Vol. 31A. Academic, London, pp. 291–326.

559 Bury, N.R., Boyle, D., Cooper, C.A., 2012. Iron. In: Wood, C.M., Farrell, A.P., Brauner, C.J.
560 (Eds.), *Fish Physiology: homeostasis and toxicology of essential metals.* Vol. 31A. Academic,
561 London, pp. 201–251.

562 Caron, A., Rosabal, M., Drevet, O., Couture, P., Campbell, P.G.C., 2018. Binding of trace
563 elements (Ag, Cd, Co, Cu, Ni, and Tl) to cytosolic biomolecules in livers of juvenile yellow

564 perch (*Perca flavescens*) collected from lakes representing metal contamination gradients.
565 Environ. Toxicol. Chem. 37, 576–586.

566 Chatterjee, A., Maiti, I.B., 1987. Purification and immunological characterization of cattish
567 Heteropneustes fossilis metallothionein. Mol. Cell. Biochem. 78, 55- 64.

568 Clearwater, S.J., Baskin, S.J., Wood, C.M., McDonald, D.G., 2000. Gastrointestinal uptake and
569 distribution of copper in rainbow trout. J. Exp. Biol. 203, 2455–2466.

570 Coleman, J.E., 1992 Zinc proteins: enzymes, storage proteins, transcription factors, and
571 replication proteins. Annu. Rev. Biochem. 61, 897–946.

572 Čanjevac, I., Orešić, D., 2015. Contemporary changes of mean annual and seasonal river
573 discharges in Croatia. Hrvat. Geogr. Glas. 77, 7-27.

574 Dragun, Z., Filipović Marijić, V., Krasnići, N., Ivanković, D., Valić, D., Žunić, J., Kapetanović,
575 D., Vardić Smrzlić, I., Redžović, Z., Grgić, I., Erk, M., 2018a. Total and cytosolic concentrations
576 of twenty metals/metalloids in the liver of brown trout *Salmo trutta* (Linnaeus, 1758) from the
577 karstic Croatian river Krka. Ecotox. Environ. Safe. 147, 537–549.

578 Dragun, Z., Krasnići, N., Kolar, N., Filipović Marijić, V., Ivanković, D., Erk, M., 2018b.
579 Cytosolic distributions of highly toxic metals Cd and Tl and several essential elements in the liver
580 of brown trout (*Salmo trutta* L.) analyzed by size exclusion chromatography and inductively
581 coupled plasma mass spectrometry. Chemosphere 207, 162–173.

582 Dragun, Z., Krasnići, N., Ivanković, D., Filipović Marijić, V., Mijošek, T., Redžović, Z., Erk,
583 M., 2020. Comparison of intracellular trace element distributions in the liver and gills of the

584 invasive freshwater fish species, Prussian carp (*Carassius gibelio* Bloch, 1782). *Sci. Total*
585 *Environ.* 730, 138923.

586 Erdogan, Z., Koc, H.T., Gungor, S., and Ulunehir, G. 2014. Age, growth and reproductive
587 properties of an invasive species *Carassius gibelio* (Bloch, 1782) (Cyprinidae) in the
588 Ikizcetepeler Dam Lake (Balikesir), Turkey. *Period. Biol.* 116(3), 285-291.

589 Festa, R.A., Thiele, D.J., 2011. Copper: an Essential Metal in Biology. *Curr. Biol.* 21, 877-883.

590 Filipović Marijić, V., Raspor, B., 2014. Relevance of biotic parameters in the assessment of the
591 spatial distribution of gastrointestinal metal and protein levels during spawning period of
592 European chub (*Squalius cephalus* L.). *Environ. Sci. Pollut. Res.* 21, (12), 7596-7606.

593 Goenaga Infante, H., Van Campenhout, K., Schaumlöffel, D., Blust, R., Adams, F.C., 2003.
594 Multi-element speciation of metalloproteins in fish tissue using size-exclusion chromatography
595 coupled “on-line” with ICP-isotope dilution-time-of-flight-mass spectrometry. *Analyst* 128, 651–
596 657.

597 Hauser-Davis, R.A., Gonçalves, R.A., Ziolli, R.L., de Campos, R.C., 2012. A novel report of
598 metallothioneins in fish bile: SDS-PAGE analysis, spectrophotometry quantification and metal
599 speciation characterization by liquid chromatography coupled to ICP-MS. *Aquat. Toxicol.* 116-
600 117, 54-60.

601 Holm, R.H., Kennepohl, P., Solomon, E.I., 1996. Structural and functional aspects of metal sites
602 in biology. *Chem. Rev.* 96, 2239-2314.

603 HRN EN 14011, 2005. Fish Sampling by Electric Power [uzorkovanje riba električnom strujom].

604 Iwasaki, Y., Saito, Y., Nakano, Y., Mochizuki, K., Sakata, O., Ito, R., Saito, K., Nakazawa, H.,
605 2009. Chromatographic and mass spectrometric analysis of glutathione in biological samples. J.
606 Chromatogr. B 877, 3309–3317.

607 Janz, D.M., 2012. Selenium. Homeostasis and Toxicology of Essential Metals. Fish Physiology
608 vol. 31A. Elsevier Inc, pp. 327–374

609 Johnson, J.L., Rajagopalan, K.V., 1976. Purification and properties of sulphite oxidase from
610 human liver. J. Clin. Invest. 58, 543-550.

611 Kammann, U., Friedrich, M., Steinhart, H., 1996. Isolation of a metal-binding protein from
612 ovaries of dab (*Limanda limanda* L) distinct from metallothionein: effect of cadmium exposure.
613 Ecotoxicol. Environ. Saf. 33, 281–286.

614 Kirschbaum, J., 1981. Cyanocobalamin. In: Florey, K. (Ed.), Analytical profiles of drug
615 substances. Vol. 10. Academic, New York, pp. 183–288.

616 Kisker, C., Schindelin, H., Rees, D.C., 1997. Molybdenum-cofactor-containing enzymes:
617 structure and mechanism. Annu. Rev. Biochem. 66, 233-267.

618 Kito, H., Tazawa, T., Ose, Y., Sato, T., Ishikawa, T., 1982. Protection by metallothionein against
619 cadmium toxicity. Comp. Biochem. Physiol. C Pharmacol. Toxicol. Endocrinol. 73, 135–139.

620 Krasnići, N., Dragun, Z., Erk, M., Raspor, B., 2013. Distribution of selected essential (Co, Cu,
621 Fe, Mn, Mo, Se and Zn) and nonessential (Cd, Pb) trace elements among protein fractions from
622 hepatic cytosol of European chub (*Squalius cephalus* L.). Environ. Sci. Pollut. Res. 20, 2340–
623 2351.

624 Krasnići, N., Dragun, Z., Erk, M., Raspor, B., 2014. Distribution of Co, Cu, Fe, Mn, Se, Zn and
625 Cd among cytosolic proteins of different molecular masses in gills of European chub (*Squalius*
626 *cephalus* L.). Environ. Sci. Pollut. Res. 21, 13512–13521.

627 Krasnići, N., Dragun, Z., Erk, M., Ramani, S., Jordanova, M., Rebok, K., Kostov, V., 2018. Size
628 exclusion HPLC analysis of trace element distributions in hepatic and gill cytosol of Vardar chub
629 (*Squalius vardarensis* Karaman) from mining impacted rivers in northeastern Macedonia. Sci.
630 Total Environ. 613-614, 1055–1068.

631 Krasnići, N., Dragun, Z., Kazazić, S., Muharemović, H., Erk, M., Jordanova, M., Rebok, K.,
632 Kostov, V., 2019. Characterization and identification of selected metal-binding biomolecules
633 from hepatic and gill cytosols of Vardar chub (*Squalius vardarensis* Karaman, 1928) using
634 various techniques of liquid chromatography and mass spectrometry. Metallomics 11, 1060–
635 1078.

636 Kryukov, G.V., Gladyshev, V.N., 2000. Selenium metabolism in zebrafish: multiplicity of
637 selenoprotein genes and expression of a protein containing 17 selenocysteine residues. Genes
638 Cells 5, 1049–1060.

639 Kuhn, D.E., O'Brien, K.M., Crockett, E.L., 2016. Expansion of capacities for iron transport and
640 sequestration reflects plasma volumes and heart mass among white-blooded notothenioid fishes.
641 Am. J. Physiol. Regul. Integr. Comp. Physiol. 311, 649–657.

642 Lavradas, R.T., Chávez Rocha, R.C., Dillenburg Saint' Pierre, T., Godoy, J.M., Hauser-Davis,
643 R.A., 2016. Investigation of thermostable metalloproteins in *Perna perna* mussels from
644 differentially contaminated areas in Southeastern Brazil by bioanalytical techniques. J. Trace
645 Elem. Med. Biol. 34, 70–78.

646 Lopez Heras, I., Palomo, M., Madrid, Y., 2011. Selenoproteins: the key factor in selenium
647 essentiality. State of the art analytical techniques for selenoprotein studies. *Anal. Bioanal. Chem.*
648 400, 1717–1727.

649 Maher, W.A., 1987. Distribution of selenium in marine animals: relationship to diet. *Comp.*
650 *Biochem. Physiol.* 86C, 131–133.

651 Martin-Antonio, B., Jimenez-Cantizano, R.M., Salas-Leiton, E., Infante, C., Manchado, M.,
652 2009. Genomic characterization and gene expression analysis of four hepcidin genes in the red
653 banded seabream (*Pagrus auriga*). *Fish Shellfish Immunol.* 26, 483–491.

654 Mason, A.Z., Jenkins, K.D., 1995. Metal detoxification in aquatic organisms. In: Tessier, A.,
655 Turner, D. (Eds.), *Metal speciation and bioavailability in aquatic systems*. IUPAC, Wiley, New
656 York, pp 479–512.

657 McGeer, J.C., Niyogi, S., Smith, D.S., 2012. Cadmium. In: Wood, C.M., Farrell, A.P., Brauner,
658 C.J. (Eds.), *Fish Physiology: Homeostasis and toxicology of nonessential metals*, vol. 31B.
659 Elsevier Academic, London, pp. 125-184.

660 Mijošek, T., Filipović Marijić, V., Dragun, Z., Ivanković, D., Krasnići, N., Erk, M., Gottstein, S.,
661 Lajtner, J., Sertić Perić, M., Matoničkin Kepčija, R., 2019a. Comparison of electrochemically
662 determined metallothionein concentrations in wild freshwater salmon fish and gammarids and
663 their relation to total and cytosolic metal levels. *Ecol. Indic.* 105, 188–198.

664 Mijošek, T., Filipović Marijić, V., Dragun, Z., Krasnići, N., Ivanković, D., Erk, M., 2019b.
665 Evaluation of multi-biomarker response in fish intestine as an initial indication of anthropogenic
666 impact in the aquatic karst environment. *Sci. Total Environ.* 660, 1079–1090.

667 Mijošek, T., Filipović Marijić, V., Dragun, Z., Ivanković, D., Krasnići, N., Redžović, Z., Sertić
668 Perić M., Vdović, N., Bačić, N., Dautović, J., Erk, M., 2020. The assessment of metal
669 contamination in water and sediments of the lowland Ilova River (Croatia) impacted by
670 anthropogenic activities. *Environ. Sci. Pollut. Res.* 27, 25374-25389.

671 Mijošek, T., Filipović Marijić, V., Dragun, Z., Ivanković, D., Krasnići, N., Redžović, Z., Erk,
672 M., 2021. Intestine of invasive fish Prussian carp as a target organ in metal exposure assessment
673 of the wastewater impacted freshwater ecosystem. *Ecol. Indic.* 122, 107247

674 NN 55, 2013. Ordinance on the Protection of Animals Used for Scientific Purposes [Pravilnik o
675 zaštiti životinja koje se koriste u znanstvene svrhe].

676 Oyoo-Okoth, E., Admiraal, W., Osano, O., Kraak, M. H. S., Gichuki, J., Ogwai, C., 2012.
677 Parasites modify sub-cellular partitioning of metals in the gut of fish. *Aquat. Toxicol.* 106-107,
678 76-84.

679 Roesijadi, G., 1992. Metallothioneins in metal regulation and toxicity in aquatic animals. *Aquat.*
680 *Toxicol.* 22, 81-114.

681 Sadler, P.J., Tucker, A., Viles, J.H., 1994. Involvement of a lysine residue in the N-terminal Ni²⁺
682 and Cu²⁺ binding site of serum albumins: comparison with Co²⁺, Cd²⁺, Al³⁺. *Eur. J. Biochem.*
683 220, 193-200.

684 Sanchez, W., Palluel, O., Meunier, L., Coquery, M., Porcher, J.M., Aît-Aïssa, S., 2005. Copper
685 induced oxidative stress in the three-spined stickleback: relationship with hepatic metal levels.
686 *Environ. Toxicol. Pharmacol.* 19, 177-183.

687 Sertić Perić, M., Matoničkin Kepčija, R., Miliša, M., Gottstein, S., Lajtner, J., Dragun, Z.,
688 Filipović Marijić, V., Krasnići, N., Ivanković, D., Erk, M., 2018. Benthos-drift relationships as
689 proxies for the detection of the most suitable bioindicator taxa in flowing waters – a pilot-study
690 within a Mediterranean karst river. *Ecotoxicol. Environ. Saf.* 163, 125–135

691 Shulgin, K.K., Popova, T.N., Rakhmanova, T.I., 2008. Isolation and purification of glutathione
692 peroxidase. *Appl. Biochem. Microbiol.* 44, 247–250.

693 Strižak, Ž., Ivanković, D., Pröfrock, D., Helmholz, H., Cindrić, A.-M., Erk, M., Prange, A.,
694 2014. Characterization of the cytosolic distribution of priority pollutant metals and metalloids in
695 the digestive gland cytosol of marine mussels: seasonal and spatial variability. *Sci. Total*
696 *Environ.* 470(471), 159–170.

697 Szpunar, J., Lobinski, R., 1999. Species-selective analysis for metal-biomacromolecular
698 complexes using hyphenated techniques. *Pure Appl. Chem.* 71, 899-918.

699 Szpunar, J., 2004. Metallomics: A new frontier in analytical chemistry. *Anal. Bioanal. Chem.*
700 378, 54-56.

701 Truglio, J.J., Theis, K., Leimkühler, S., Rappa, R., Rajagopalan, K.V., Kisker, C., 2002. Crystal
702 structures of the active and alloxanthine inhibited forms of xanthine dehydrogenase from
703 *Rhodobacter capsulatus*. *Structure* 10, 115-125.

704 Uchida, H., Kondo, D., Yamashita, A., Nagaosa, Y., Sakurai, T., Fujii, Y., Fujishiro, K., Aisaka,
705 K., Uwajima, T., 2003. Purification and characterization of an aldehyde oxidase from
706 *Pseudomonas* sp. KY 4690. *FEMS Microbiol. Lett.* 229, 31–36.

707 Urien, N., Jacob, S., Couture, P., Campbell, P.G.C., 2018. Cytosolic distribution of metals (Cd,
708 Cu) and metalloids (As, Se) in livers and gonads of field-collected fish exposed to an
709 environmental contamination gradient: an SEC-ICP-MS analysis. *Environments* 5 (102), 1–17.

710 van Campenhout, K., Goenaga Infante, H., Goemans, G., Belpaire, C., Adams, F., Blust, R.,
711 Bervoets, L., 2008. A field survey of metal binding to metallothionein and other cytosolic
712 ligands in liver of eels using an on-line isotope dilution method in combination with size
713 exclusion (SE) high pressure liquid chromatography (HPLC) coupled to inductively coupled
714 plasma time-of-flight mass spectrometry (ICP-TOFMS). *Sci. Total Environ.* 394, 379–389.

715 van Campenhout, K., Goenaga Infante, H., Hoff, P.T., Moens, L., Goemans, G., Belpaire, C.,
716 Adams, F., Blust, R., Bervoets, L., 2010. Cytosolic distribution of Cd, Cu and Zn, and
717 metallothionein levels in relation to physiological changes in gibel carp (*Carassius auratus*
718 *gibelio*) from metal-impacted habitats. *Ecotoxicol. Environ. Safe.* 73, 296–305.

719 Vidal, S.M., Malo, D., Vogan, K., Skamene, E., Gros, P., 1993. Natural resistance to infection
720 with intracellular parasites: isolation of a candidate for Bcg. *Cell* 73, 469–485.

721 Vijver, A.G., van Gestel, C.A.M., Lanno, R.P., van Straalen, N.M., Peijnenburg, W.J.G.M.,
722 2014. Internal metal sequestration and its ecotoxicological relevance: a review. *Environ. Sci.*
723 *Technol.* 38, 4705–4712.

724 Vutukuru, S.S., Chintada, S., Madhavi, K.R., Rao, J.V., Anjaneyulu, Y., 2006. Acute effects of
725 copper on superoxide dismutase, catalase and lipid peroxidation in the freshwater teleost fish,
726 *Esomus danricus*. *Fish Physiol. Biochem.* 32, 221–229.

727 Walker, R.L., Fromm, P.O., 1976. Metabolism of iron by normal and iron deficient rainbow
728 trout. *Comp. Biochem. Physiol.* 55A, 311–318.

729 Wallace, W.G., Lee, B.-G., Luoma, S.N., 2003. Subcellular compartmentalization of Cd and Zn
730 in two bivalves. I. Significance of metal-sensitive fractions (MSF) and biologically detoxified
731 metal (BDM). *Mar. Ecol. Prog. Ser.* 249, 183–197.

732 Watanabe, T., Kiron, V., Satoh, S., 1997. Trace minerals in fish nutrition. *Aquaculture* 151, 185-
733 207.

734 Yamashita, Y., Yamashita, M., 2010. Identification of a novel selenium-containing compound,
735 selenoneine, as the predominant chemical form of organic selenium in the blood of a bluefin
736 tuna. *J. Biol. Chem.* 285, 18134-18138.

737

738

739

740

741

742

743

744

745

746 **Figure captions:**

747 **Figure 1.** Distribution profiles of two selected elements (Cd: a-d; Cu: e-h) among cytosolic
748 biomolecules of different molecular masses in the intestine of brown trout from the two sites of
749 the Krka River (Krka River source and Town of Knin) and Prussian carp from the two sites of
750 the Ilova River (Ilova village and Trebež village) in two seasons (autumn and spring)

751 **Figure 2.** Distribution profiles of two selected elements (Co: a-d; Fe: e-h) among cytosolic
752 biomolecules of different molecular masses in the intestine of brown trout from the two sites of
753 the Krka River (Krka River source and Town of Knin) and Prussian carp from the two sites of
754 the Ilova River (Ilova village and Trebež village) in two seasons (autumn and spring)

755 **Figure 3.** Distribution profiles of two selected elements (Mo: a-d; Se: e-h) among cytosolic
756 biomolecules of different molecular masses in the intestine of brown trout from the two sites of
757 the Krka River (Krka River source and Town of Knin) and Prussian carp from the two sites of
758 the Ilova River (Ilova village and Trebež village) in two seasons (autumn and spring)

759 **Figure 4.** Distribution profiles of Zn among cytosolic biomolecules of different molecular
760 masses in the intestine of brown trout from the two sites of the Krka River (Krka River source
761 and Town of Knin) and Prussian carp from the two sites of the Ilova River (Ilova village and
762 Trebež village) in two seasons (autumn and spring)

763

Table 1. Dissolved trace element concentrations in the water ($\mu\text{g L}^{-1}$, mean \pm S.D.; $<$ LOD values) of the Krka and Ilova rivers at reference (Krka River source and Ilova village) and contaminated sites (Town of Knin and Trebež village) in two seasons (autumn and spring).

	Krka River				Ilova River			
	Krka River source		Town of Knin		Ilova village		Trebež village	
	Autumn	Spring	Autumn	Spring	Autumn	Spring	Autumn	Spring
Cd ($\mu\text{g L}^{-1}$)	0.010 \pm 0.003	0.005 \pm 0.001	0.010 \pm 0.004	0.005 \pm 0.002	0.011 \pm 0.006	0.006 \pm 0.002	0.053 \pm 0.003	0.035 \pm 0.002
Co ($\mu\text{g L}^{-1}$)	$<$ 0.019	$<$ 0.019	0.196 \pm 0.010	0.211 \pm 0.033	0.137 \pm 0.005	0.320 \pm 0.006	0.121 \pm 0.011	0.338 \pm 0.009
Cu ($\mu\text{g L}^{-1}$)	$<$ 0.401	$<$ 0.401	$<$ 0.401	$<$ 0.401	0.400 \pm 0.028	0.687 \pm 0.075	0.716 \pm 0.030	0.678 \pm 0.071
Fe ($\mu\text{g L}^{-1}$)	0.910 \pm 0.370	4.04 \pm 0.31	4.88 \pm 0.37	5.16 \pm 0.85	17.89 \pm 2.17	21.81 \pm 1.95	21.58 \pm 1.52	20.78 \pm 5.89
Mo ($\mu\text{g L}^{-1}$)	0.210 \pm 0.004	0.378 \pm 0.087	0.410 \pm 0.005	0.515 \pm 0.032	0.561 \pm 0.027	0.611 \pm 0.010	0.981 \pm 0.062	0.724 \pm 0.039
Se ($\mu\text{g L}^{-1}$)	0.080 \pm 0.022	$<$ 0.059	0.100 \pm 0.014	0.088 \pm 0.059	0.786 \pm 0.019	0.596 \pm 0.016	1.01 \pm 0.11	0.485 \pm 0.015
Zn ($\mu\text{g L}^{-1}$)	$<$ 7.34	11.07 \pm 5.02	20.41 \pm 5.15	17.87 \pm 1.26	$<$ 7.34	$<$ 7.34	$<$ 7.34	$<$ 7.34

Table 2. Biometric characteristics and cytosolic trace element concentrations in the intestine of 12 specimens of brown trout (*Salmo trutta* Linnaeus, 1758) from the Krka River and 12 specimens of Prussian carp (*Carassius gibelio* Bloch, 1782) from the Ilova River used for analyses of intestinal trace element distributions.

Site	Sample ID	Total length/cm	Total mass/g	Sex	Cd	Co	Cu	Fe	Mo	Se	Zn	
					$\mu\text{g kg}^{-1}$	$\mu\text{g kg}^{-1}$	mg kg^{-1}	mg kg^{-1}	$\mu\text{g kg}^{-1}$	mg kg^{-1}	mg kg^{-1}	
Krka River	K2	27.0	201.7	M	15.1	28.1	0.432	11.96	49.7	0.712	55.6	
	Krka River	K5	27.8	194.2	F	107.1	42.2	0.336	11.55	31.0	0.802	39.0
	source - autumn	K11	27.5	175.0	F	6.15	8.76	0.155	8.59	17.3	0.362	52.7
		K53	22.1	107.2	M	11.13	5.31	0.210	2.00	22.0	0.691	26.2
	Krka River	K67	17.0	50.6	F	271.3	17.1	0.493	5.88	32.6	0.705	37.4
	source - spring	K68	16.5	46.7	F	24.3	11.1	0.390	5.14	33.5	0.655	40.2
		K20	23.9	146.0	F	47.6	121.3	1.348	8.54	43.2	1.784	46.5
	Town of Knin -	K21	25.5	193.0	M	21.6	45.5	0.348	12.20	27.0	1.302	36.4
	autumn	K26	16.2	53.7	M	8.76	48.4	0.884	2.49	40.0	1.587	27.9
		K42	22.6	122.2	M	2.25	38.4	0.588	8.70	26.4	0.996	50.5

Ilova River	Town of Knin -	K46	20.5	102.4	M	4.77	23.4	0.272	4.52	19.7	1.064	53.4
	spring	K47	19.1	84.9	M	6.93	81.0	0.253	5.62	21.5	1.017	61.5
		IL57	17.9	99.3	F	259.1	25.6	0.480	10.05	71.2	0.538	111.8
	Ilova village -	IL65	17.1	83.4	F	387.2	16.1	1.043	9.37	58.5	0.377	84.3
	autumn	IL68	19.9	136.2	F	133.0	17.7	0.782	9.45	62.5	0.403	102.3
		IL116	18.2	71.2	M	30.9	33.8	0.816	17.58	64.3	/	126.4
	Ilova village -	IL118	18.7	82.1	M	41.8	28.1	0.358	8.27	49.5	0.389	105.3
	spring	IL121	17.7	68.1	M	25.1	33.8	0.427	8.51	58.2	0.474	147.2
		IL72	18.5	112.3	F	564.4	11.3	0.812	14.92	68.2	0.470	75.9
	Trebež village -	IL76	23.7	239.3	F	683.8	15.1	1.060	22.03	48.1	0.414	76.2
	autumn	IL81	20.5	139.6	M	753.0	33.1	1.361	/	81.8	0.560	96.7
		IL94	17.1	96.2	F	129.2	39.9	0.818	12.47	56.7	0.499	139.6
	Trebež village -	IL96	26.6	316.7	F	100.5	29.0	0.908	14.39	70.7	0.447	123.4
	spring	IL100	27.2	339.2	F	220.5	18.8	1.332	12.42	51.9	0.445	108.0

Table 3. Elution times (t_e) and molecular masses (MM) of eight proteins used as standards for calibration of Superdex 200 10/300 GL size exclusion column, as well as of rabbit metallothionein standard (Enzo Metallothionein-1, Enzo Metallothionein-2).

Equation of calibration straight line was: $K_{av} = -0.277 \times \log MM + 1.627$.

	Protein	t_e	MM	Concentration
		/ min	/ kDa	/ mg mL⁻¹
Superdex 200 10/300 GL	Thyroglobulin	16.12	669	8
	Apo-ferritin	17.88	443	10
	β -amylase	20.55	200	4
	Alcohol dehydrogenase	21.8	150	5
	Bovine albumin	23.06	66	10
	Superoxide dismutase	27.71	32	1.25
	Carbonic anhydrase	29.60	29	3
	Metallothionein - 2	31.22	6.1	1
	Metallothionein - 1	32.32	6.1	1
	Vitamin B12	36.14	1.35	3

Table 4. Elution times (t_e) and molecular masses (MM) of cytosolic proteins from intestine of brown trout (*Salmo trutta* Linnaeus, 1758) from the Krka River and of Prussian carp (*Carassius gibelio* Bloch, 1782) from the Ilova River contained within the fractions (obtained by separation of cytosols using SEC-HPLC with Superdex 200 10/300 GL column) in which respective elements were eluted. Presented data refer to maxima of trace element peaks (i.e. to fractions with the highest trace element concentrations), whereas the numbers within the brackets refer to the beginnings and the ends of trace element peaks.

Element	Location	^a HMM peak 1		^a HMM peak 2		^b MMM peak		^c LMM peak		^d VLMM peak 1		^d VLMM peak 2		
		t_e / min	MM / kDa	t_e / min	MM / kDa	t_e / min	MM / kDa	t_e / min	MM / kDa	t_e / min	MM / kDa	t_e / min	MM / kDa	
Cd	Krka River							30,31 (28-38)	18,14 (30-24)					
	Ilova River							32 (29-37)	11 (24-3)					
Co	Krka River			22 (20-24)	141 (235-85)	25 (24-28)	65 (85-30)				33,35 (30-38)	8,5.1 (18-24)	41 (39-44)	1.1 (1.8-0.5)
	Ilova River			22,23 (19-24)	141,109 (303-85)	26 (24-28)	51 (85-30)				36,37 (30-38)	3,9.3 (18-24)	41 (39-43)	1.1 (1.8-0.7)
Cu	Krka River					26, 27 (24-28)	51, 39 (85-30)	30,31 (28-36)	18,14 (30-3.9)					
	Ilova River					28 (26-30)	30 (51-18)	32 (30-37)	11 (18-3)					

Fe	Krka River	17,18 (14-21)	506,392 (1088-182)			25,26 (23-28)	65,51 (109-30)	33 (31-37)	8 (14-3)	36 (32-39)	39 (11-1.8)		
	Ilova River	18,19 (16-22)	392,303 (653-141)			27 (26-30)	39 (51-18)	33 (31-35)	8 (14-5.1)				
Mo	Krka River			19,20 (18-22)	303,235 (392-141)					35 (33-39)	5.1 (8-1.8)		
	Ilova River			20 (18-23)	235 (392-109)					35 (33-39)	5.1 (8-1.8)		
Se	Krka River									36 (35-39)	3.9 (5.1-1.8)	41,42 (40-45)	1.1,0.8 (1.4-0.4)
	Ilova River			23 (19-28)	109 (303-30)					36,37 (32-39)	3.9,3 (11-1.8)	42 (40-45)	0.8 (1.4-0.4)
Zn	Krka River	15,16 (14-18)	843,653 (1088-392)	23,24 (20-28)	109,85 (235-30)								
	Ilova River	15 (14-18)	843 (1088-392)	23 (20-28)	109 (235-30)					36,37 (31-39)	3.9,3 (14-1.8)	40 (39-43)	14 (1.8-0.7)

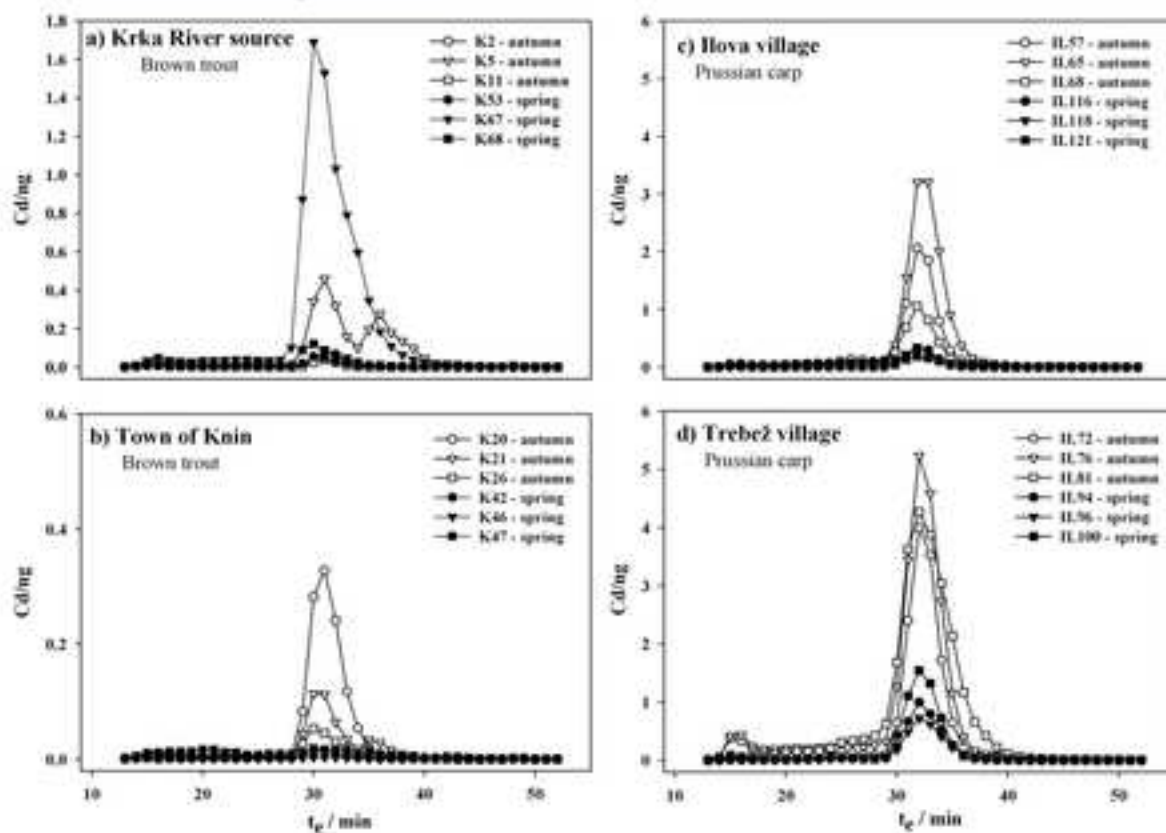
^aHMM peak – a peak of trace element concentration in the cytosolic fractions with a maximum in high molecular mass protein region (>100 kDa)

^bMMM peak – a peak of trace element concentration in the cytosolic fractions with a maximum in medium molecular mass protein region (30-100 kDa)

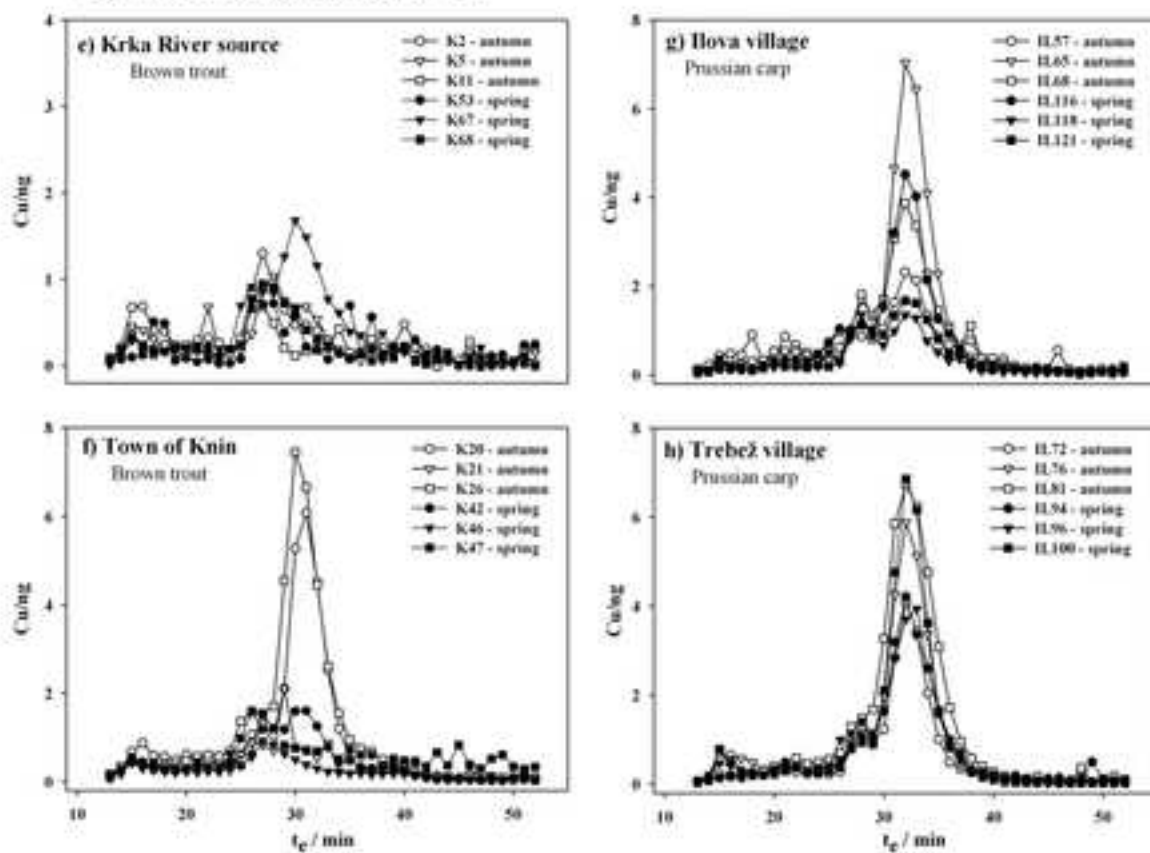
^cLMM peak – a peak of trace element concentration in the cytosolic fractions with a maximum in low molecular mass protein region (10-30 kDa)

^dVLMM peak – a peak of trace element concentration in the cytosolic fractions with a maximum in very low molecular mass protein region (<10 kDa)

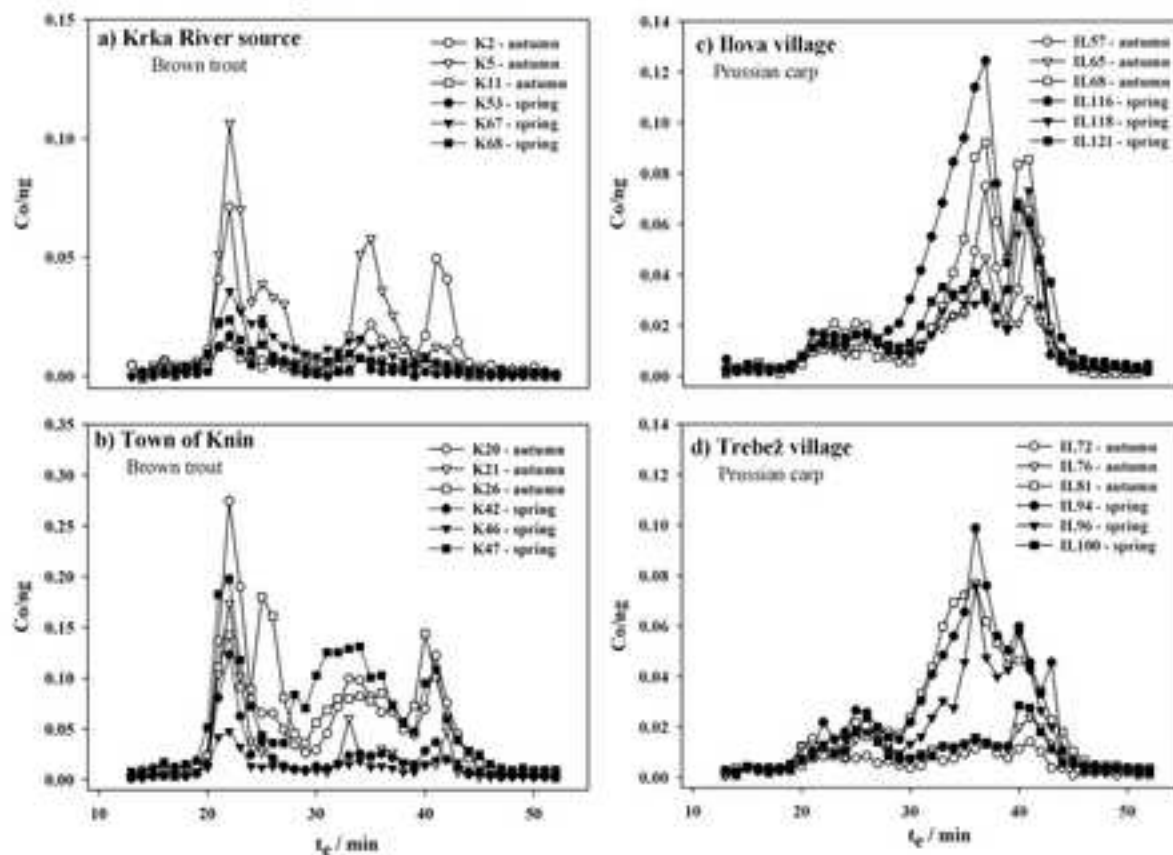
Distribution profiles of Cd



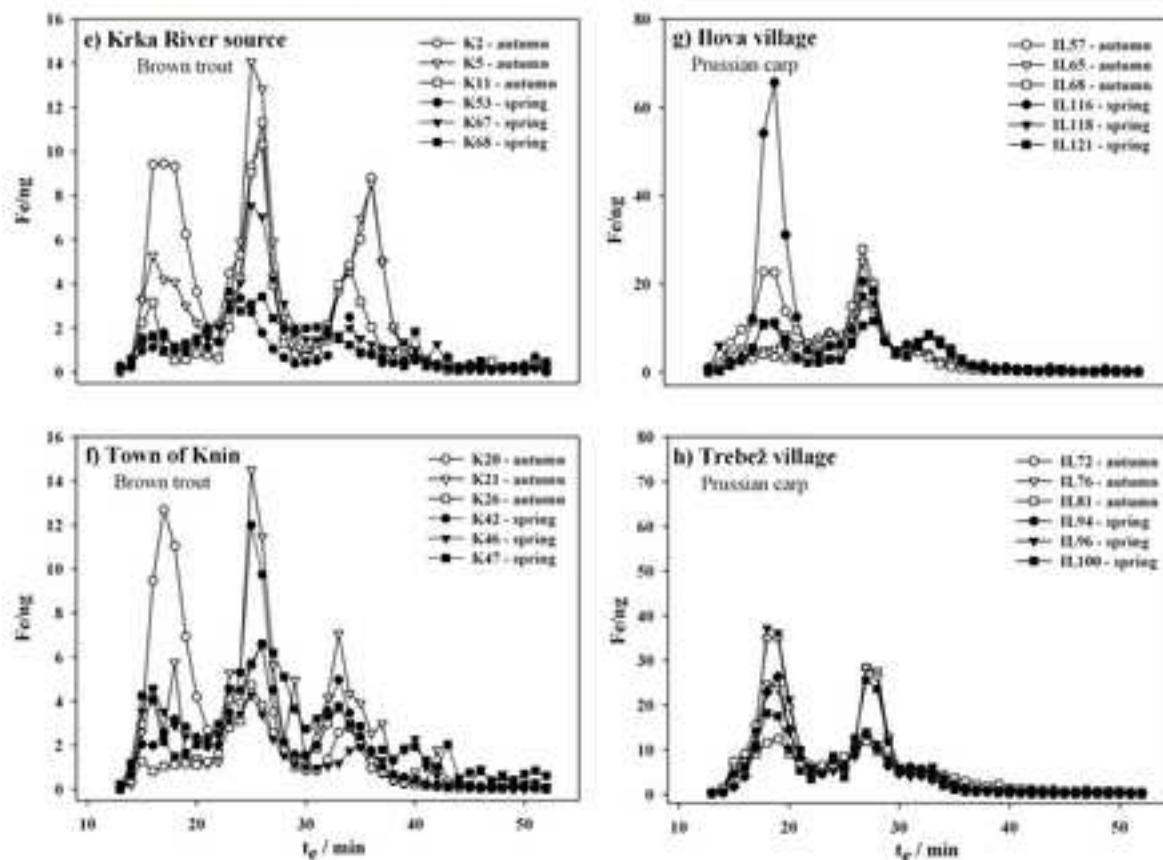
Distribution profiles of Cu



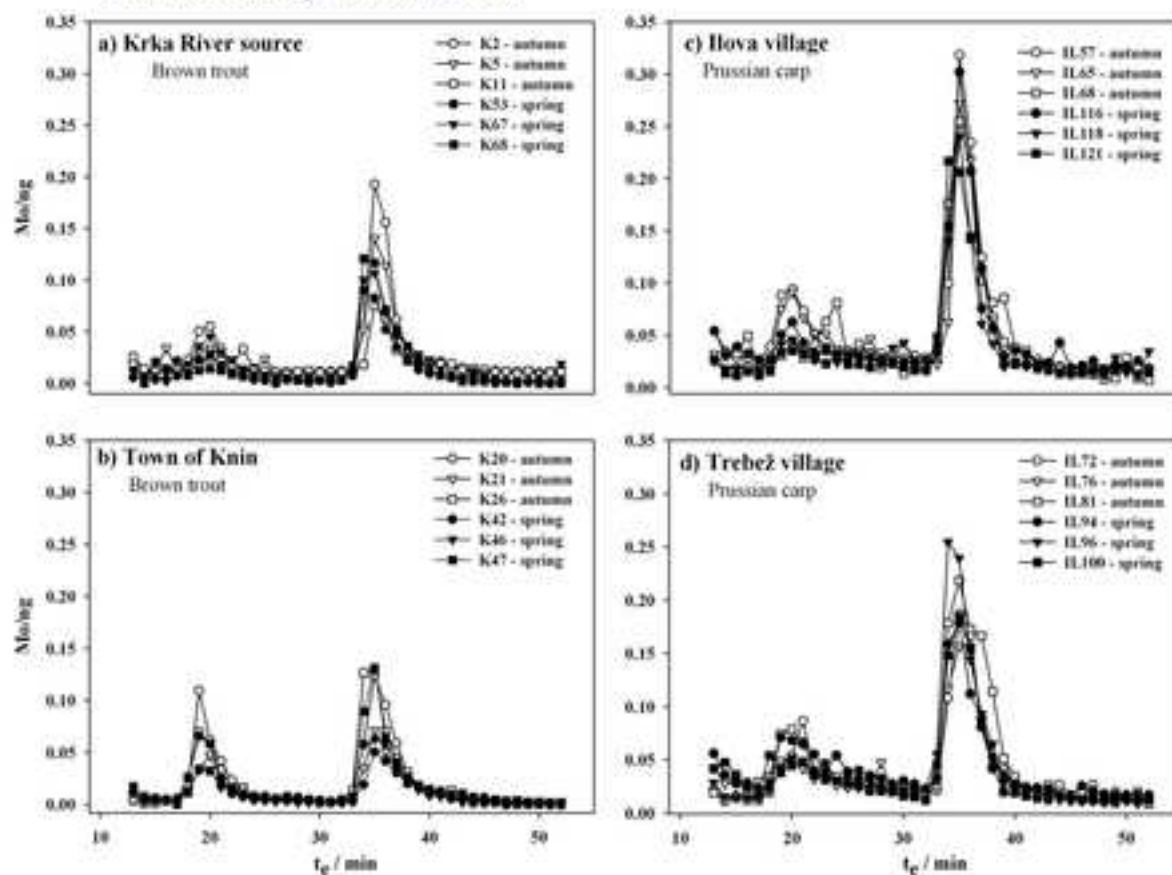
Distribution profiles of Co



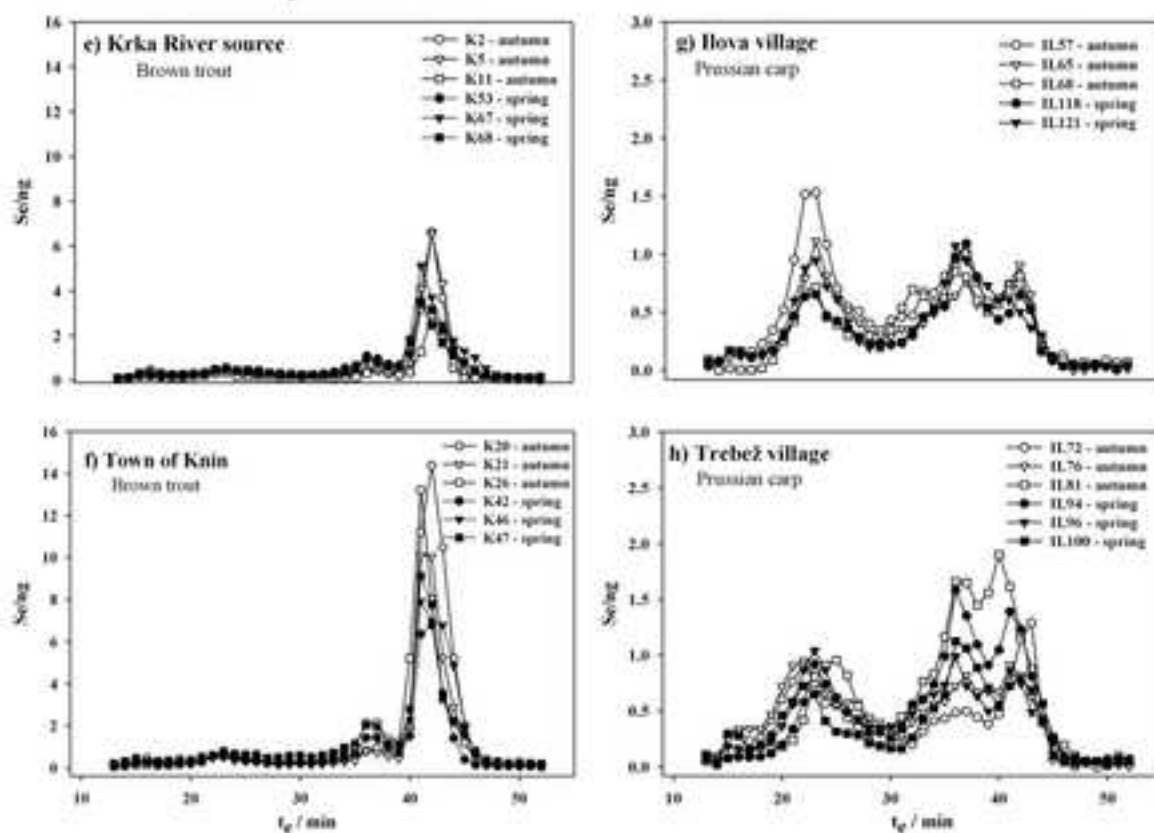
Distribution profiles of Fe



Distribution profiles of Mo



Distribution profiles of Se



Distribution profiles of Zn

